PCCP

PAPER

View Article Online
View Journal | View Issue

Cite this: *Phys. Chem. Chem. Phys.*, 2019, **21**, 26606

Librating dipoles as a probe of spontaneously electrical films and as a source of THz radiation

D. Field

Received 22nd October 2019,
Accepted 25th November 2019

DOI: 10.1039/c9cp05746c

rsc.li/pccp

Pulsed electrical excitation of films, composed of spontaneously oriented dipolar molecules, is predicted to cause libration of the constituent species about their fixed lattice sites, accompanied by an oscillating surface potential and emission of THz radiation. We focus on a 100 monolayer (ML) film of nitrous oxide, deposited at 53.5 K, containing oriented dipoles which sustain a spontaneous field of 4.77×10^7 V m^{-1} and an associated surface potential of 1.386 V. An external field of 10^8 V m^{-1}, applied to the film, perturbs the angle of dipole orientation by $\sim 0.95^\circ$. Rapid removal of this field causes the dipoles to librate about their steady state orientation. The surface potential oscillates accordingly with a peak-to-peak amplitude of 0.587 V and a frequency of 2.090 THz. The librational motion of the dipoles generates 1.409 μW of THz power per cm^2 of substrate, in 4π sr, composed of short bursts of radiation, at a repetition frequency of 4.181 THz. This power may be generated effectively continuously if the perturbing field is applied at a frequency of a few kHz. Observation of the amplitude and time structure of oscillatory surface potentials and of THz emission may potentially provide new and general probes of the spontelectric state, allowing direct observation of hindered molecular rotation and revealing the range of angles of dipole orientation in the crystalline environment.

1. Introduction

The formation of thin cryo-films of polar molecules, by condensation from the gas phase at sufficiently low temperature, may lead to material composed of spontaneously dipole-oriented species. Such 'spontelectric' films possess associated bulk electric fields, which can exceed 10^8 V m^{-1}.[1–4] The spontelectric effect is a widespread phenomenon and examples of molecules which form polarized films are diverse, including such species as nitrous oxide (N_2O), *cis*-methyl formate, chloro-fluoro-hydrocarbons and toluene.[3] Electric fields within films depend on their temperature of deposition. This lies at the root of the sensitivity to temperature of IR spectra[5–7] and VUV spectra of solid films,[4,8] respectively through the vibrational Stark effect and the effect of an electric field on excitons in the solid. The spontelectric effect also gives a new handle on the study of the process of crystallization and phase change in general, *via* neutron scattering studies.[9,10]

The surface potential at the film/vacuum interface for spontelectric films, and the corresponding electric field within these films, has been shown to be proportional to the degree of dipole orientation.[3] The latter is defined as the ratio of the projection of the average dipole, to the normal to the film, to the total dipole moment of the molecule in the solid state (Section 2). Application of an external electric field induces changes in the degree of dipole orientation of the constituent species, through the additional torque induced on the molecular dipoles. We envisage that an external field be ramped up such that the system can fully adjust to the associated perturbation, creating a new steady-state, with a modified molecular orientation and surface potential. We now propose that the perturbing electric field be rapidly removed. The molecular dipole orientation relaxes towards its field-free value and this is predicted to generate 'spontelectric libration', in which the constituent dipoles reverberate about their steady state orientation. The surface potential responds accordingly, reflecting the libratory motion. Spontelectric libration, essentially the hindered rotation of dipoles, will be accompanied by the emission of radiation at THz frequencies.

In Section 2, we calculate the trajectory of a dipole as it rotates to re-assert its field-free, steady-state spontelectric orientation, on abrupt removal of the applied field. Timescales for this motion are found to be of the order of 10^{-13} seconds, for librations corresponding to rotations of $\sim 1^\circ$. In Sections 3 and 4, the form of the oscillation of the surface potential on the film is calculated and it is shown that libration of the constituent dipoles gives rise to readily measureable emission of THz radiation of the order of microwatts to nanowatts,[11] per 100 monolayers (ML) per cm^2 of film. Moreover, films may ring like a bell for several milliseconds after the initial pulse excitation. In Section 5, we describe how the amplitude of the applied electric

Department of Physics and Astronomy, University of Aarhus, Aarhus, DK-8000, Denmark. E-mail: dfield@phys.au.dk

field, and its pulsed removal, dictates the frequency of THz emission and its power. In this work, we introduce the new phenomena of externally induced libration in spontelectrics and accompanying emission of THz radiation, relating these features to the nature of the spontelectric state. Discussion is limited to the single example of nitrous oxide as a spontelectric material.

Conventional molecular libration has been observed in both Raman spectroscopy[12–14] and in FIR (or THz) absorption experiments,[11,15] the latter in films of solid N_2O. Librational frequencies lie between 2 THz and 3.6 THz, associated with rotations of half-angle of order of $\sim 2^\circ$, given harmonic motion.[13] In Section 4, we use data from ref. 13 in order to estimate the extent of homogeneous broadening in the system.

Table 1 Parameters for N_2O: eqn (1)–(4). $\langle E_S\rangle$, $\langle E_A\rangle$ and ζ control the spontelectric characteristics of electric field and degree of dipole orientation, $\langle\mu\rangle/\mu_0$, for temperatures of deposition, $T > 48$ K.[9] The value of the layer spacing, s, in N_2O is taken from neutron scattering data.[9] α is the isotropic molecular polarizability, μ_g and μ_0 are the gas phase and solid state dipole moments, respectively. The moment of inertia, I, enters into the dynamics of libration through eqn (5)

N_2O
$\langle E_S\rangle = 6.01 \pm 0.22 \times 10^8$ V m^{-1}
$\langle E_A\rangle = 6.39 \pm 0.25 \times 10^8$ V m^{-1}
$\zeta = 57.5 \pm 3.9$
$\alpha = 3.31 \times 10^{-30}$ m^3
$s = 0.2905 \pm 0.002$ nm
$\mu_g = 0.166$ D
$\mu = 0.0667$ D
Moment of inertia, $I = 6.699 \times 10^{-46}$ kg m^2

2. Formulation of the model: imposition of an external field and the dipole trajectory

We use a parametrized mean field model of the spontelectric state, described in detail in ref. 3. This model has been has been shown to reproduce the temperature dependence of observed spontelectric fields in solid films of nitrous oxide, nitrous oxide diluted in xenon, *cis*-methyl formate (*cis*-MF) and CCl_xF_y ($x + y = 4$). The model provides an analytical description of the counter-intuitive behaviour of *cis*-MF, in which dipole orientation is found to increase with temperature of film deposition above ~ 77 K. The model also underpins a description of the observed deposition temperature dependence of IR and VUV spectra of films of N_2O, *cis*-MF, CO and NH_3.[4–7,16]

The electric field in the film of material, in which the component of the field at any moiety, in the z-direction normal to the plane of the film, E_z, is written as the sum of parts symmetric and asymmetric in z, as described in detail in ref. 3. The asymmetric term gives rise to the spontelectric field. The degree of dipole orientation is given by $\langle\mu\rangle/\mu_0$, where μ_0 is the total dipole moment of the molecule, modified by its environment in the solid state, and $\langle\mu\rangle$ is its average z-component. Thus $\cos^{-1}(\langle\mu\rangle/\mu_0)$ is the angle of orientation, θ, of the dipole to the vertical. All dipoles are treated as equivalent. We note that net components of dipole orientation in the x–y plane of the film are zero, reflecting the lack of azimuthal dependence of the orientation. The characteristic of the spontelectric state is that $\langle\mu\rangle/\mu_0$ is non-zero.

E_z is written as:

$$E_z = \langle E_S\rangle[1 + \zeta(\langle\mu\rangle/\mu_0)^2] - \langle E_A\rangle(\langle\mu\rangle/\mu_0) \quad (1)$$

where $\langle E_S\rangle$, $\langle E_A\rangle$ and ζ are parameters taken to be independent of deposition temperature, over any temperature range for which there is no abrupt structural change.[9] Note that the value of $\langle E_A\rangle$ is given by $\mu/\varepsilon_0\Omega$,[3] where Ω is the molecular volume (= 37.79 Å^3 for N_2O[9]). Thus $\langle E_A\rangle$ is fixed and not a free parameter for solid N_2O; see Table 1. The $\zeta(\langle\mu\rangle/\mu_0)^2$ term in eqn (1) may be interpreted as a measure of the tendency of one dipolar species to restrict the angular motion of another, a so-called 'frustration' term, whose strength is governed by the value of the free parameter ζ. The asymmetric term, $\langle E_A\rangle\langle\mu\rangle/\mu_0$, arising from the long-range polarization, gives the value of the observed spontelectric field within the film, illustrating the linear dependence of the surface potential on the degree of dipole orientation.

Mean field theory gives an implicit expression for $\langle\mu\rangle/\mu_0$, yielding the familiar Langevin function for orientational interactions:[3,17]

$$\frac{\langle\mu\rangle}{\mu_0} = \coth\left(\frac{E_z\mu_0}{T}\right) - \left(\frac{E_z\mu_0}{T}\right)^{-1} \quad (2)$$

Combining eqn (1) and (2) yields an implicit expression for $\langle\mu\rangle/\mu_0$,

$$\langle\mu\rangle/\mu_0 = -T/\{\mu[\langle E_S\rangle(1 + \zeta(\langle\mu\rangle/\mu_0)^2) - \langle E_A\rangle(\langle\mu\rangle/\mu_0) - E_w]\} + \coth\{\mu[\langle E_S\rangle(1 + \zeta(\langle\mu\rangle/\mu_0)^2) - \langle E_A\rangle(\langle\mu\rangle/\mu_0) - E_w]/T\} \quad (3)$$

An externally applied electric field is included in eqn (3), through the presence of an independent parameter, E_w, defining the perturbing field. This is simply added to the unperturbed value of E_z in eqn (1) and taken here as negative (see below). The dipole moment of a molecule in the solid state is expressed as[3,18]

$$\mu_0 = \mu_g/(1 + \alpha k/s^3) \quad (4)$$

where 's' is the average spacing between successive layers, α is the isotropic molecular polarizability, $k = 11.034$[19] and μ_g is the gas phase dipole moment of the molecule involved. We note that the tensor nature of the polarizability should strictly be included in evaluating μ_0. However, a straightforward relationship equivalent to eqn (4) for molecular depolarization in solids, but including the tensor nature of the polarizability, is not available. Indeed, only a detailed quantum chemical model could yield a suitably modified value of μ_0. We make the assumption here that this value would not differ greatly from the value estimated using eqn (4).

Eqn (2) and all subsequent numbered equations are expressed in atomic units for notational simplicity. Parameters for N_2O are shown in Table 1.

In the analysis which follows, discussion is limited to a single illustrative case, that of N_2O at a deposition temperature of 53.5 K, chosen in the mid-range of the validity of the parameters in Table 1, valid for 48 K to 60 K.[9] A standard value of the parameter for the applied field, E_w, of 10^8 V m^{-1} is initially adopted. Variation of E_w is discussed in Section 5. In the absence of E_w, the degree of dipole orientation, $\langle\mu\rangle/\mu_0 = 0.0747$.[9] For $E_w = 10^8$ V m^{-1}, a numerical solution of eqn (3) yields $\langle\mu\rangle/\mu_0 = 0.05824$. Thus the application of an external field places the average dipole in a new steady state, suppressing the degree of dipole orientation in accordance with Le Chatelier's principle, for the sign of E_w chosen throughout, that is, in the direction of the spontelectric field. Application of the field in the opposite sense, not discussed further here, causes the degree of dipole alignment to increase. The imposition of E_w therefore rotates the dipole orientation in the system, as mentioned in the introduction. Note that, with the parameters in Table 1, the value in eqn (1) of the term $\langle E_S\rangle(1 + \zeta(\langle\mu\rangle/\mu))^2$ is 7.94×10^8 V m^{-1} and that of the spontelectric field $\langle E_A\rangle\langle\mu\rangle/\mu_0$ is 4.77×10^7 V m^{-1}, for comparison with E_w. The value of the laboratory potentials, necessary to generate $E_w = 10^8$ V m^{-1}, would be dictated by the geometry of any experimental set-up, but would not require more than a few volts.

We now consider the effects which will ensue if E_w is removed to zero though application of an external pulse, which acts to null the applied field. The pulse must be of sufficiently short fall-time, t_r, that the process results in no energy transfer to the surroundings. On this criterion, t_r should be a few to a few tens of ps or, in order to preserve temporal integrity in any experiment, as close as feasible to the inherent 0.1 ps timescale associated with the motion of the dipoles, derived below. We return briefly to the aspect of experimental feasibility in Section 6. At all events, for experimentally realistic values of $t_r > 0.1$ ps, the first quarter cycle of the rotational trajectory of the dipoles will be dictated by the form of a relatively slow decay of the field. This aspect does not however vitiate any future experiment. It is in principle immaterial to the molecular rotational energy, acquired as E_w is removed, whether this is engendered by the direct action of a realistic and slowly falling field or through storage of the energy of the field in a non-steady state created through a fictively small removal time of the perturbing field. This invariance arises because the amount of energy imparted to the dipoles is equal in both cases, provided the change is sufficiently rapid such as to allow for no energy transfer to the surroundings. Thus the rotational energy of the dipoles, at the end of the first quarter cycle of rotation, is unaffected by the fall time of the perturbing field to zero. The acquisition of rotational energy takes place on a corresponding expanded timescale, in a manner which in practice reflects the form of the changing electric field in the medium. We are therefore free to ignore this initial part of the trajectory and proceed as if the perturbation, introduced through E_w, were removed on the order of $<10^{-13}$ s timescale. In this connection, the rotation (or libration) of the dipoles in the first few cycles in a real system will cause only negligible emission of radiation, upholding the condition for negligible energy loss. We also note that removal of a field of 10^8 V m^{-1} will cause molecular cooling of <0.1 K, which would have an insignificant effect on the system.[3]

The above scheme, of applying a field and then removing it rapidly, creates a network of oriented dipoles which will spontaneously relax as a coherent ensemble, with a small in-built delay of $\sim$0.15 fs, for a film of thickness of 100 ML considered below. For our illustrative standard case, of a film deposited at 53.5 K, relaxation takes place from an initial angle of orientation $\cos^{-1}$ 0.05824, that is, $\theta_i = 1.5125$ at $E_w = 10^8$ V m^{-1} towards the $E_w = 0$ value, corresponding to the unperturbed spontelectric state, with an angle of orientation $\theta_s = \cos^{-1}$ 0.07469 = 1.4960, known from experiment.[3] This motion amounts to a rotation of 0.0165 radians or 0.95°. The dipoles will then continue to rotate through a further small and similar angle, to be determined, and then return on an oscillatory trajectory, as we describe below. We consider the effects of a distribution in the initial values of angle of orientation in Section 4.

We now work towards the determination of how the rate of change with time of the angle of orientation, $\omega = d\theta/dt$, itself changes with time, t. Thus to connect ω and t, we need to put together ω *vs.* θ with θ *vs.* t, where the latter is effectively the waveform of the surface potential. Analysis of the dynamics must moreover be performed for a complete cycle of the motion of the dipole. We start by considering motion between $\theta_i = 1.5125$ and $\theta_s = 1.4960$, the first quarter of one cycle.

The torque on an average molecule is given by its moment of inertia, I, times the angular acceleration, $d^2\theta/dt^2$. This torque is due to the net electric field on the dipole, given by the difference between E_z in eqn (1) for $\langle\mu\rangle/\mu_0$ in the state engendered in the presence of the applied field, *via* the parameter E_w, and the unperturbed spontelectric state in the absence of any applied field. We make the approximation that the resulting rotational motion introduces no centrifugal distortion and therefore that the moment of inertia remains constant during relaxation of the dipole orientation. Thus,

$$\frac{d^2\theta}{dt^2} = \frac{\mu}{I}\Big\{\Big\{\langle E_S\rangle[1 + \zeta(\langle\mu\rangle/\mu_0)^2] - \langle E_A\rangle(\langle\mu\rangle/\mu_0)\Big\}\sin\theta - \langle E_S\rangle[1 + \zeta(\langle\mu\rangle_s/\mu_0)^2] - \langle E_A\rangle(\langle\mu\rangle_s/\mu_0)\sin\theta_s\Big\} \quad (5)$$

Since values of θ are close to $\pi/2$ and, in order to simplify the algebra, we use $\sin(\pi/2 - \theta) \sim (\pi/2 - \theta)$, where this approximation yields values which may be shown to give a vanishingly small difference from the exact form. We then obtain:

$$\frac{d^2\theta}{dt^2} = -\frac{\mu(\theta - \theta_s)}{8I}\{\{\langle E_A\rangle[3\pi(\pi - 2(\theta + \theta_s) + 4(\theta^2 + \theta\theta_s + \theta_s^2 - 2)] - 2\langle E_S\rangle(\pi - (\theta + \theta_s)) \times [2 + (\pi^2 - 2\pi(\theta + \theta_s))] + 2(\theta^2 + \theta_s^2 - 2))]\zeta\}\} \quad (6)$$

The right-hand side (rhs) of eqn (6) depends only on the single variable, θ. We seek the time, t, required for the rotation of the

dipole, from the initial angle θ_i, in the presence of an applied field, to any $\theta \leq \theta_s$, the unperturbed spontelectric value. Writing Θ as the rhs of eqn (6), t is then a solution of $\int\int d^2\theta/\Theta = \int\int dt^2$, for the appropriate limits of θ, that is, θ_i and any value of θ. The constants of integration are determined from the boundary conditions that $\theta = \theta_i$ for $t = 0$ and that ω, the rotational velocity = $d\theta/dt = 0$ at $t = 0$, the instant at which E_w falls to zero. Imposition of these boundary conditions, yields a time t, to move from an initial value of θ_i to any value of θ, given by:

$$t = \{2[h(\theta) - h(\theta_i)(\theta/\theta_i)]\}^{1/2} \quad (7)$$

where $h(\theta)$ is obtained by double integration of Θ^{-1} and may be expressed as

$$h(\theta) = \sum_{j=1}^{j=4} (a_j + b_j\theta) \ln\left[(c_j - \theta)^2\right] \quad (8)$$

where a_j, b_j and c_j are determined by values of the dipole moment of the molecule in the solid, μ_0, the moment of inertia, I and the spontelectric parameters $\langle E_A \rangle$, $\langle E_S \rangle$ and ζ in eqn (1). Note that there are no loss mechanisms included in the above analysis, which would contribute to damping of the motion. We return to this point below.

In order to give some physical insight into this analysis, we note first that the acceleration declines in absolute value from $t = 0$ onwards, from a maximum at $\theta = \theta_i$ to zero at $\theta = \theta_s$. The latter property is clearly indicated through the multiplier on the rhs of eqn (6). Thus the motion is sluggish at first, that is with $\theta = \theta_i$, starting from a velocity of the angle of orientation, ω (= $d\theta/dt$) = 0, but with maximum acceleration. The velocity continues to increase until $\theta = \theta_s$, at which point ω reaches a maximum and becomes asymptotically constant with time. The value of ω is itself given by the value of $(dt/d\theta)^{-1}$ obtained from eqn (7), substituting for $h(\theta)$ using eqn (8). Using parameters for N_2O in Table 1 and a deposition temperature of 53.5 K, yields the variation of ω with θ shown in Fig. 1, noting that rotation of the dipole is represented by a decline in the value of θ. Strictly therefore the angular velocity, ω, is a negative quantity.

Eqn (7) establishes the relationship between t and θ. This is illustrated in Fig. 2, where time, on the vertical axis, *versus* angle of orientation passes through a point of inflection at $\theta = \theta_s$, marking the end of the first quarter cycle of libration of the dipole. Fig. 2 shows that the time to perform the first quarter cycle of 0.0165 radians is 1.196×10^{-13} seconds, for the standard film. Comparison with rotation in the gas phase gives a time of 1.566×10^{-14} seconds for the same extent of rotation, in $J = 6$, the most populated level at 53.5 K. Thus rotation in the solid state is, as expected, more hindered than free rotation in the gas phase.

Moving beyond $\theta = \theta_s$, the acceleration changes sign and the rotor slows down until it reaches the end point of its libration. At this stage the process is reversed, the dipole returns through $\theta = \theta_s$ and, within this model involving zero energy loss, continues on its trajectory until it reverts to $\theta = \theta_i$. Libratory motion would continue indefinitely, were the energy loss

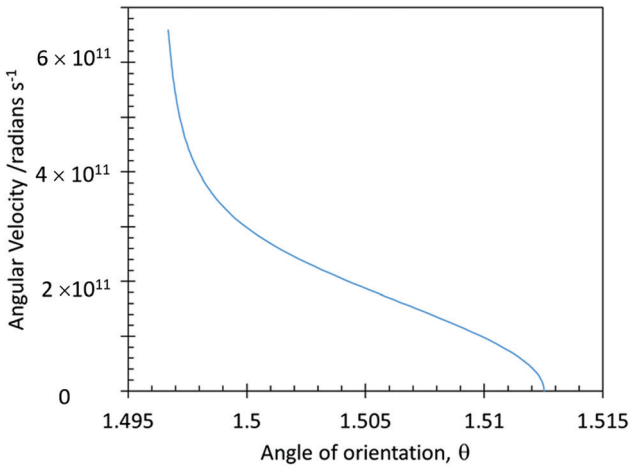

Fig. 1 The variation of the angular velocity, ω, with the angle of orientation θ of the N_2O dipoles, for the standard film deposited at 53.5 K, over the first quarter cycle of libration. The initial angle θ_i = 1.5125 corresponds to the degree of orientation when the applied field, E_w, = 10^8 V m^{-1}. The unperturbed spontelectric value of θ_s = 1.4960 marks the end of the first quarter cycle. Table 1 gives values of spontelectric and other parameters used here.

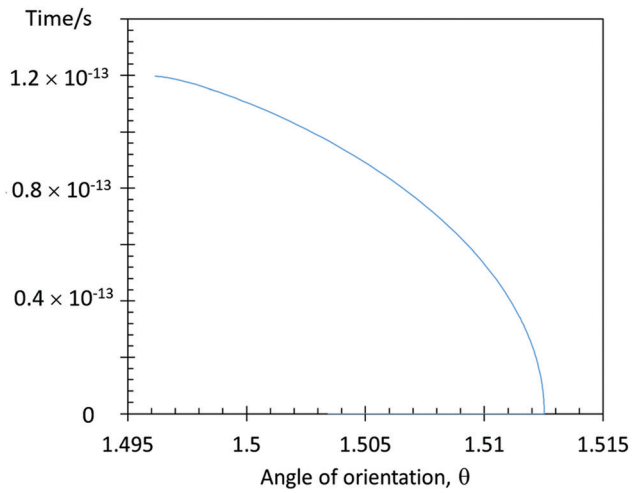

Fig. 2 The variation with time of the angle of orientation, between θ_i = 1.5125 corresponding to $E_w = 10^8$ V m^{-1} and θ_s = 1.4960, for E_w = 0, of constituent molecules of N_2O in a thin film deposited at 53.5 K, with time on the vertical axis, following rapid removal of an applied field of $E_w = 10^8$ V m^{-1}. See Table 1 for values of spontelectric and other parameters.

mechanism, through emission of radiation from the rotating dipole, not to intervene. It turns out, as we show below, that this loss mechanism becomes significant only after $>10^9$ cycles have been performed. For this reason, the dynamics is discussed below without this additional complication. In addition, no other loss mechanisms, for example through coupling into low energy lattice modes, are included here.

The potential which governs the torque is asymmetrical about θ_s, the unperturbed spontelectric value. Thus motion of the dipole beyond θ_s is not precisely a mirror image of that illustrated in Fig. 1 and 2. In order to find the destination value of $\theta = \theta_d$, achieved at the end of the first half cycle, we impose

the condition that the amount of work performed by the field on the dipole in the first quarter cycle, in rotating from θ_i to θ_s, must be equal to the amount of work, performed by the dipole against the field, in rotating from θ_s to θ_d in the second quarter cycle. The work done is the integral of the electric field with respect to θ, with the relevant limits, multiplied by the dipole moment, and is given by:

$$\int d\theta \Big[-\frac{\mu(\theta - \theta_s)}{8I} \{ \{ \langle E_A \rangle [3\pi(\pi - 2(\theta + \theta_s)] + 4\big(\theta^2 + \theta\theta_s + \theta_s^2 - 2\big)\big] - 2\langle E_S \rangle (\pi - (\theta + \theta_s))\big[2 + \big(\pi^2 - 2\pi(\theta + \theta_s)\big)\big] + 2\big(\theta^2 + \theta_s^2 - 2\big)\big]\zeta \} \} \Big] \quad (9)$$

where the limits are θ_i, θ_s and θ_s, θ_d for the first and second quarter cycles respectively. Since we know θ_i and θ_s, the only unknown is θ_d and equating the two integrals with limits θ_i, θ_s and θ_s, θ_d, yields $\theta_d = 1.4808$. Thus in the first quarter cycle the average dipole rotates through $\theta_i - \theta_s = 0.01648$ radians and in the second quarter through $\theta_s - \theta_d = 0.01520$ radians, reflecting the asymmetry of the system inherent in eqn (3). This analysis yields the second quarter of the trajectory, equivalent to that in Fig. 2. The variation of θ with time which emerges for the first half cycle is shown in Fig. 3, displayed as θ *vs.* time. The inset to Fig. 3 shows two and a half complete cycles of the librational motion of the dipole, that is, the waveform of the motion.

The surface potential, given by $\langle E_A \rangle \langle \mu \rangle / \mu_0$ multiplied by the thickness of the film, will oscillate in harmony with the value of θ.

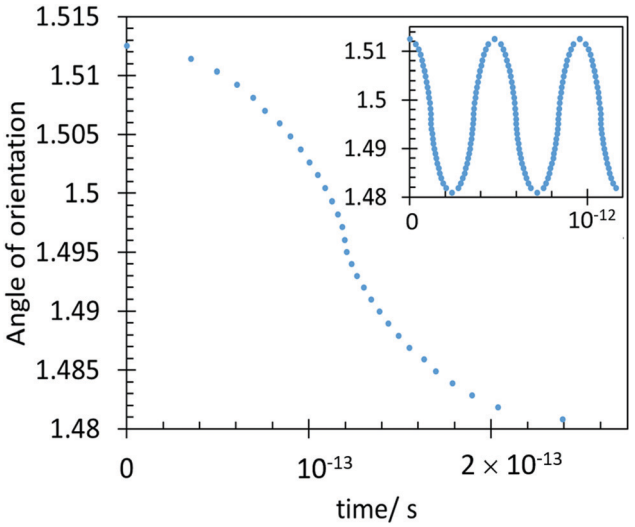

Fig. 3 The variation with time in the first half cycle of the angle of orientation of the dipole to the vertical, normal to the film surface, for a film of N_2O deposited at 53.5 K, following excitation through removal of an applied field. Time zero (t = 0) represents the moment at which this applied field, equal to $E_w = 10^8$ V m^{-1} (eqn (3)), is switched off. The inset shows two and a half complete cycles of the librational motion of the dipole. The electric field in the film follows this waveform with values given by cosine of the angle of orientation × $\langle E_A \rangle$; see eqn (1). The surface potential follows the same form, with a value given by the field × the thickness of the film = 29.05 nm in the standard 100 ML film (see text).

Thus the field within the film oscillates between 5.744×10^7 V m^{-1} and 3.724×10^7 V m^{-1} and the surface potential will oscillate with a peak-to-peak amplitude of 0.587 V with a frequency of 2.090 THz, reflecting the period of the libration shown in the inset to Fig. 3. We note in passing that if any associated power could be coupled out with a suitable device, *via* the substrate, the excited film may constitute a source of THz radiation. At all events, the film will act as an antenna without further intervention, launching a THz wave train from the librating dipole. We now estimate how much power could be generated by the film, ignoring any substrate effect. In this connection, the substrate could be chosen to be an insulator, since neither the spontelectric effect nor its strength depends on the nature of the substrate.[3,20]

3. Generation of THz emission

The total power output of radiation into 4π sr of a dipole rotating at angular frequency $\omega = d\theta/dt$ is given by $\mu^2\omega^4/(6\pi\varepsilon\varepsilon_0 c^3)$ in SI units.[21] We write ω as a function of time = $g_1(t)$ and $g_2(t)$, for the first and second quarter cycles respectively. Since we have imposed the condition that the amount of work exchanged between the field and the dipole is equal in the first and second quarter cycles, strictly we need only consider a single quarter cycle. However as a test of numerical results, we have chosen to consider the two quarter cycles separately and to compare the figures that emerge.

In order to proceed, we require the forms of $g_1(t)$ and $g_2(t)$. These are conveniently obtained from data given in Fig. 3, where ω is given by the local slope, $d\theta/dt$, for any θ. We find that the variation of ω with time, shown in Fig. 3, accurately follows a power law of the form $g_1(t) = \alpha_1 + \alpha_2(t_1 - t)^{1/1.75} + \alpha_3(t_1 - t)^{1/3} + \alpha_4(t_1 - t)^{1/5} + \alpha_5(t_1 - t)^{1/7} + \alpha_6(t_1 - t)^{1/9}$ for the first quarter cycle and $g_2(t) = \beta_1 + \beta_2(-t_1 + t)^{1/1.75} + \beta_3(-t_1 + t)^{1/3} + \beta_4(-t_1 + t)^{1/5} + \beta_5(-t_1 + t)^{1/7} + \beta_6(-t_1 + t)^{1/9}$ for the second quarter cycle, where α_i and β_i are determined from least squares fitting. Here, t_1 is the time taken to move between the initial and final angles, θ_i and θ_s, in the first quarter cycle, that is, 1.196×10^{-13} seconds (Fig. 2).

We note that we previously derived the variation of ω with θ, shown in Fig. 1. For any chosen value of θ, we can therefore obtain a value of ω. For any value of θ we can also assign a value of time, t, using eqn (7) and (8). Self-consistency requires that, if we now insert this value of t into the power law $g_1(t)$, we recover the same value of ω. We find that this is satisfied to a fraction of a percent throughout the range of ω, t and θ encountered here.

As a further check on the foregoing analysis, we now impose the condition that the energy associated with rotational motion, acquired as described above, must equal the energy injected into the system by the applied electric field, since this is the energy lost on its rapid removal from the system. For the first quarter cycle, the energy associated with rotational motion is given by the integral over time of $\frac{1}{2}I\omega^2$, that is, $\frac{1}{2}I\int g_1(t)^2 \cdot [dg_1(t)/dt] \cdot dt$ between $t = 0$ and t_1. Equating this integral with the energy gained by the system from the imposed electric field, given by the integral in

eqn (9), omitting the moment of inertia, yields the time, t_1. Thus, we solve:

$$\int_{\theta_i}^{\theta_s} d\theta \Big[-\frac{\mu(\theta-\theta_s)}{8} \{\langle E_A\rangle[3\pi(\pi-2(\theta+\theta_s)+4(\theta^2+\theta\theta_s+\theta_s^2-2)] -2\langle E_S\rangle(\pi-(\theta+\theta_s))[2+(\pi^2-2\pi(\theta+\theta_s))]+2(\theta^2+\theta_s^2-2))]\zeta\}\Big] = \tfrac{1}{2}I\int_0^{t_1} g_1(t)^2[dg_1(t)/dt]dt \quad (10)$$

for t_1. We find that the value of t_1 so obtained is indeed equal to the value of 1.196×10^{-13} seconds, just mentioned, given through integration of eqn (6) and shown in Fig. 2 for $\theta = \theta_s$. We also find that the total energy gained on rotating from θ_i = 1.5125 to θ_s = 1.4960 is 1.235×10^{-25} J per rotor and that an essentially identical result is obtained on analysing the second quarter cycle, that is, on integrating from θ_s to θ_d on the left-hand side (lhs) of eqn (10) and t_1 to t_2 on the rhs, using $g_2(t)$ to replace $g_1(t)$. The above analysis shows that the fitted functions $g_1(t)$ and $g_2(t)$ are accurate representations of the form of $\omega(t)$.

The radiant energy emitted in the first quarter cycle, P_1, is given by

$$P_1 = 2\mu^2/(3\varepsilon c^3)\int_0^{t_1} g_1(t)^4[dg_1(t)/dt]dt \quad (11)$$

where all quantities are expressed in atomic units. A similar expression for P_2 is given by the integral over t_1 to t_2 using $g_2(t)$, where t_2 is the time required to achieve $\theta = \theta_d$ = 1.4808, the destination value for a half cycle of the libratory motion of the dipole, as determined above. We ignore any dispersion in the medium in the frequency range of interest of 1 to 15 THz (see Section 5). The value of ε is therefore taken to be the static value of $1 + \alpha k/s^3 = 2.489$,[8,22] using data for N_2O from Table 1. Evaluation of P_1 and P_2 shows that we satisfy the necessary condition that P_1 is numerically equal to P_2 to better than 1 part in 10^5. Note that films of material considered here are optically thin to the passage of THz radiation.[15]

We now estimate the THz power that a film may deliver. The total power, P_{total}, in one complete cycle in 4π sr, is given by,

$$P_{total} = 4\left[2\mu^2/(3\varepsilon c^3)\int_0^{t_1} g_1(t)^4[dg_1(t)/dt]dt\right]N_{rot}(2f) \quad (12)$$

that is, 4 times the integral in eqn (11), times the number of rotors in the film, N_{rot}, times the twice the frequency of the libration of the dipole (f = 2.0904 THz), since 2 pulses are emitted per cycle of libration, associated with each of the two points of inflection (see inset to Fig. 3). The approximation is made here is that the power is continuously sustainable, to which we return below. The number of rotors, N_{rot}, for a standard 100 ML sample, of area 1 cm^2, layer spacing s = 0.2905 nm (Table 1, ref. 9), is 1.18×10^{17}. This yields an output power, P_{total}, of 1.4096 μW. In passing, for comparison, the power in black body radiation at 53.5 K, the film deposition temperature, at a frequency of 4.181 THz is 1.624×10^{-18} W in 4π sr per Hz. Thus the power emitted is equal to that of black body radiation in a bandwidth of 0.867 THz.

We turn now to the angular distribution of the THz radiation created by the rotating dipoles in the system, ignoring any classical interference effects (see below), treating the system as effectively a single emitter. Dipole rotation takes place in a plane containing the z-axis. Thus the maximum emission will be in a direction perpendicular to this plane and the minimum will lie in this plane, following the relationship $(1 + \cos^2\chi)$.[21] Here χ is the polar angle in the coordinate system attached to the direction of the molecular dipole. There is no azimuthal dependence of the emission due to the net zero dipole orientation in the xy-plane of the film. Hence the maximum emission will lie in a direction in the plane of the film, but offset by the angle of orientation. Since the angles, χ, lie on an axis system fixed on the molecular orientation, it would therefore in principle be possible to measure the dipole orientation, $\langle\mu\rangle/\mu_0$, from the asymmetrical distribution of power measured in the laboratory. We note that the angular dependence of the emission is not strongly constrained to be close to the xy-plane. Thus in the solid angle contained within (say) $\chi = 60^\circ$ to 120°, that is, looking at the film in plan view, the proportion of the total emission is $\sim$0.12. Note that through a simple multiplication by N_{rot} in eqn (12), interference effects between radiation emitted by different dipoles are ignored. The film will however behave as a 3D coherently phased array, yielding an interference pattern associated with N_{rot} emitting dipoles.[23] Near-field effects may result in modification of the angular distribution of emitted radiation,[24] an aspect to be considered in future work.

Evidently if the system loses power at the rate of 1.4096 μW, as estimated above, this limits the lifetime of the motion which gives rise to THz emission. As noted, we have ignored this contribution to the dynamics and we now examine the validity of this approximation. The energy supplied to our standard film, composed of 1.18×10^{17} molecules, through application of a field parameter of 10^8 V m^{-1}, is 1.235×10^{-25} J per molecule (see back) and thus 1.457×10^{-8} J in total. This energy is lost at a rate of 1.4096×10^{-6} J s^{-1} and the entire power would therefore be dissipated in $\sim$10 ms. Thus the approximation in our analysis, that the loss of power due to emission of radiation may be ignored in the analysis of the dynamics, is valid if the sample is pulsed, and the process of libration reinitiated, at a frequency of a few kHz to yield an effectively continuous output. Values of power are subsequently expressed in Watts, in which it is understood that the cycle of excitation of the film is repeated at kHz frequencies to maintain a constant output.

4. Temporal form of THz emission

We consider now the factors that govern the temporal form of the THz output for the standard film. To summarize, we have estimated that a film of N_2O deposited at 53.5 K, on removal of an applied field of 10^8 V m^{-1}, creates radiation at a frequency of 4.181 THz, for some milliseconds or effectively continuously if

suitable pumped. This radiation consists of pulses whose peaks are separated by 2.392×10^{-13} seconds, each formed as the system performs the trajectory shown in Fig. 3. These pulses will however be broadened by both homogeneous and inhomogeneous effects.

Turning first to homogeneous broadening, we propose here that a simple indication of the temporal form of emission would be to treat it as Lorentzian with some characteristic width $1/(\pi T_2)$, where T_2 is a relaxation time characteristic of the entire ensemble of species.[25] Essentially, we introduce random noise, that is, fluctuating forces, into the system to simulate the quantum effect of homogeneous broadening.[26] In order to estimate the degree of this broadening, we use Raman spectroscopy data from ref. 13 for N_2O at 70 K, which shows a linewidth of 7 cm^{-1}. On this basis, each pulse, with a repetition rate of 4.181 THz, would be 0.21 THz in width.

Inhomogeneous broadening will by contrast give rise to a spread in the value of the centre frequency of 4.181 THz. This effect turns on the distribution of angles associated with dipole orientation, since emission frequency depends on θ_i, the initial angle of orientation. The range of angles may be estimated from experimental data in ref. 3 to possess an upper limit ± 0.0007 FWHM. Using this limit, a population of species with θ_i differing from the standard median value of $\langle\mu\rangle/\mu_0 = 0.07469$ by ± 0.0007, that is by $\pm \sim 0.04^\circ$, would give rise to an increase of pulse width of ~ 4 fs twice per cycle, on the basis of the analysis presented in Section 2. Evidently, as time after removal of the external field progresses, emission yields an overall waveform which broadens and flattens, to an extent which depends critically on the unknown distribution of θ_i.

For the present, we may conclude that measurements of the output from pulsed spontelectric films could be reverse-engineered to yield information on both the environment of molecules in the solid, relating to homogeneous effects, and the distribution of angles in which molecules point in spontelectric films, relating to inhomogeneous effects.

5. Dependence of THz emission frequency on the strength of the applied pulsed field

We show here how the emission frequency can be tuned by adjusting E_w. In order to keep the analysis as transparent as possible, we have chosen to make a numerical approximation to eqn (2), Section 2, setting $\mathrm{Coth}(x) \approx x/3$, the first term in the expansion of this function. This allows the implicit form of eqn (3) to be relaxed and yields an analytical relationship between $\langle\mu\rangle/\mu_0$ and E_w:

$$\langle\mu\rangle/\mu_0 = [\langle E_A\rangle\mu + 3T - \sqrt{(\langle E_A\rangle\mu + 3T)^2 + 4\mu^2\langle E_S\rangle\zeta(E_w - \langle E_S\rangle)}\,]/(2\mu\langle E_S\rangle\zeta) \quad (13)$$

For the case of $E_w = 0$ and inserting the relevant parameters from Table 1, eqn (13) yields $\langle\mu\rangle/\mu_0 = 0.07532$, that is, 1% higher than the exact value of 0.07469 given by eqn (3). Equally, using $E_w = 10^8$ V m^{-1}, eqn (13) yields $\langle\mu\rangle/\mu_0 = 0.05842$ which may be compared with the value of 0.05824 obtained without recourse to the current approximation for $\mathrm{Coth}(x)$. Eqn (13) may be rewritten for the angle of orientation, θ, as

$$\theta = \frac{\pi}{2} - \frac{\left[\langle E_A\rangle\mu + 3T - \sqrt{(\langle E_A\rangle\mu + 3T)^2 + 4\mu^2\langle E_S\rangle\zeta(E_w - \langle E_S\rangle)}\right]}{2\mu\langle E_S\rangle\zeta}$$
$$= 1.475 + 283.6\sqrt{7.594 \times 10^{-8} + 1.849 \times 10^{-4}E_w} \quad (14)$$

where we have used the approximation, adopted in Section 2, that $\sin(\pi/2 - \theta) \sim (\pi/2 - \theta)$ and thus that $\theta = \pi/2 - \langle\mu\rangle/\mu_0$, since $\theta = \cos^{-1}\langle\mu\rangle/\mu_0$. Eqn (14) is also expressed in terms of the numerical values associated with the relationship between θ and E_w, using parameters in Table 1. Eqn (14) yields the dependence of the initial condition of $\theta = \theta_i$ on the value of E_w. Essentially we have re-expressed the boundary condition for $\theta = \theta_i$ explicitly in terms of E_w. Eqn (14) may then be inserted into eqn (7) and (8), yielding the dependence on E_w of the time, t_1, to move from an initial value of θ_i to θ_s. The inverse of $2t_1$ then gives the frequency of the THz emission, as in described Section 3, and thus its relation to E_w.

Fig. 4 shows the variation the frequency of the emitted THz radiation as a function of E_w between 10^7 V m^{-1} and 2×10^8 V m^{-1}. This illustrates that the frequency of THz emission increases as E_w falls. A lower limit of $E_w = 10^7$ V m^{-1} is chosen in Fig. 4, because the linearization of the coth function becomes increasingly inaccurate for smaller E_w, for example

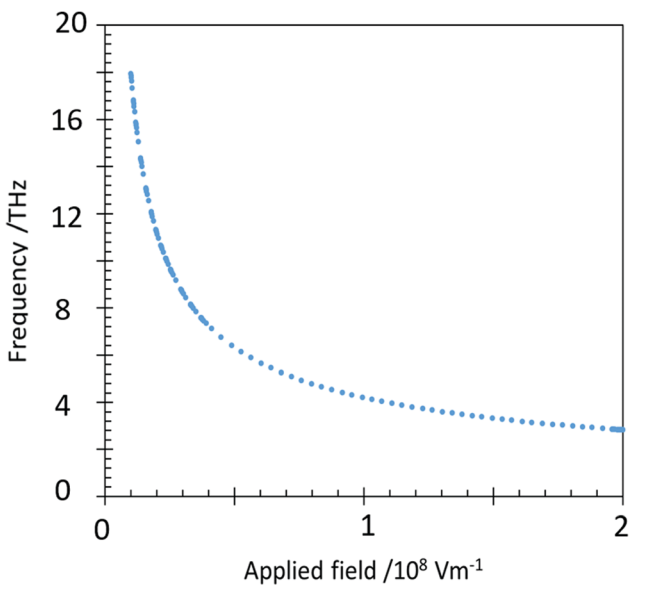

Fig. 4 The variation of the frequency of THz emission *vs.* the amplitude of the pulsed applied field, E_w, emitted from a film of solid N_2O deposited at a temperature of 53.5 K.

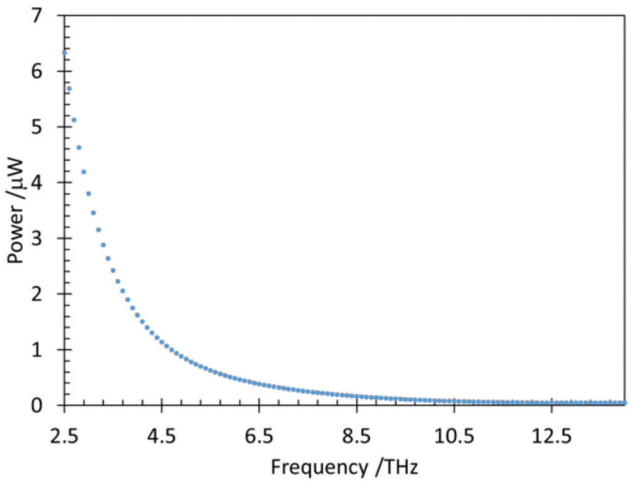

Fig. 5 The relationship between emitted power in μW, in 4π sr, for the standard film and frequency in THz. Selected values are shown in Table 2. Area of N_2O film = 1 cm^2, thickness 100 ML and temperature of deposition 53.5 K.

yielding an overestimate of ~10% for the computed frequency of emission at $E_w = 10^7$ V m^{-1}.

Modification of E_w will be accompanied by a modified total power emitted, following excitation of the spontelectric film. Since the energy added to the system is proportional to E_w^2, the total emitted power will follow accordingly, where the total power is the sum of emission over all time. This however includes the decaying tail of emission, in which decay becomes significant after ~10 ms for the standard conditions of $E_w = 10^8$ V m^{-1} (Section 3). We do not treat this decay in the present work, but concentrate here on the total power behaviour, in the early time regime up to a few ms after the removal of E_w. This implies that the cycle of excitation of the film is repeated at kHz frequencies, as mentioned in Section 3.

The radiant energy emitted in the time t_1, that is, in the first quarter cycle, is given by the integral on the lhs of eqn (10). This integral may be evaluated for values of θ_i corresponding to chosen values of E_w between, say, 2×10^8 V m^{-1} and 1.5×10^7 V m^{-1}, with θ_i obtained from a solution of eqn (3) using $\theta = \pi/2 - \langle\mu\rangle/\mu_0$. Using the dependence θ_i on E_w, eqn (14), we may therefore estimate the early time THz power for our standard 1 cm^2 100 ML film, as a function of E_w, where early time signifies the first few ms of emission for which decay of the dipole oscillation may be ignored. Since we know the variation of the frequency of the emitted THz radiation as a function of E_w (Fig. 4), this yields the early time power as function of frequency. The resulting variation of THz power with frequency may be found in Fig. 5, showing a rapid drop in output as frequency increases. Thus at 13.53 THz, corresponding to $E_w = 1.5 \times 10^7$ V m^{-1}, output is 0.0403 μW whereas at 2.83 THz, corresponding to $E_w = 2 \times 10^8$ V m^{-1}, the power is 4.475 μW. Some representative values are given in Table 2.

Table 2 Power *vs.* frequency of emission for the standard spontelectric film, area 1 cm^2, thickness 100 ML of N_2O laid down at 53.5 K. Column 1: values of emitted power, into 4π sr, in the first few ms after pulse excitation. Column 2: the corresponding frequency of emission. Column 3: amplitude of the field associated with film excitation, E_w. In order to maintain the power shown, the sample must be excited at kHz frequencies. Graphical data for power *vs.* frequency are shown in Fig. 5

Power in 4π sr/μW	Frequency/THz	Corresponding E_w/V m^{-1}
0.0403	13.53	1.5×10^7
0.108	9.708	2.5×10^7
0.403	6.332	5×10^7
0.846	4.973	7.5×10^7
1.409	4.203	10^8
2.073	3.696	1.25×10^8
2.769	3.331	1.5×10^8
3.619	3.054	1.75×10^8
4.475	2.834	2×10^8

6. Concluding comments

It remains a challenge to study the forces that bind together the molecular constituents of solid materials. The direct observation of oscillating surface potentials in spontelectrics, and the related time structure of associated THz emitted power, may serve to probe these forces, in particular relation to the topics (i), (ii) and (iii) below.

(i) The observation of hindered molecular rotation in the solid state, relating to melting and phase change in general. Spontelectric libration provides a means of monitoring rotational motion rather directly, *via* the oscillating surface potential and associated THz emission. Experiments could for example be performed in the vicinity of the phase change in N_2O at around 47–48 K[9] or at deposition temperatures associated with decay of the spontelectric effect, that is, at temperatures close to the so-called Curie point for spontelectrics. An example of the latter would be isoprene (2-methyl-1,3-butadiene, C_5H_8) between 70 K and 80 K,[3] in which large fluctuations in the angles of dipole orientation are expected to occur and barriers to relative rotational motion are overcome.

(ii) The mechanism of large-scale self-organisation in spontelectrics. Self-organisation leads to spontaneous dipole orientation, but the mechanism remains unknown. It has been suggested that it may be fluctuation driven.[27] Observations of the temporal behaviour of libration as a function of deposition temperature should shed light on how the counter-intuitive spontelectric phenomenon takes hold and how it can be so readily initiated by simple deposition from the gas phase.[3]

(iii) The homogeneity of the environment within crystalline structures and the inhomogeneity of the medium, the latter in terms of the range of angles of dipole orientation within self-organized structures: the time structure of emitted pulses at THz frequencies would provide quantitative information on both these topics.

With respect to the feasibility of the observation of THz radiation, rapid removal of the field may be achieved using fast pulse generators with sub-10 ps switching times. THz bolometry provides more than adequate sensitivity at the power levels predicted here.[11,28] Photoconductive switching may additionally be employed to reduce switching times, using

techniques developed in the field of terahertz time-domain spectroscopy (THz-TDS).[29,30] The perturbing field, E_w, may be set up using a mesh, which may be tailored to allow transmission of THz radiation.[31] We note that the generation of THz radiation described in the present work is distinct from the general run of methods of production of THz radiation.[11,32] Here we envisage a purely electrical method of THz generation, in contrast to methods using a photoconductive antenna,[33] involving excitation using a femtosecond laser pulse. The active medium, of a simple film of vacuum-deposited species, is also very straightforward to prepare in comparison with the Ga, As, Al alloy heterostructures employed in quantum cascade sources.[34] We naturally recognize that the requirement for cryogenics, and restrictions on emitted power, may limit the widespread use of spontelectrics as the basis of a THz emission device.

The current work remains conceptual, but referring back to the physics in (i), (ii) and (iii) above and to paraphrase a well-known slogan, the observation of spontelectric libration through accompanying THz signals, promises to 'reach parts which other methods cannot reach'. This work may therefore be regarded as a blueprint for future experiments. Observations of the oscillation of the surface potential and of the emitted THz radiation show potential to see inside solid materials and to explore the molecular environment in crystalline and partially disordered materials in a novel manner.

Conflicts of interest

There are no conflicts to declare.

Acknowledgements

I should like to thank Peter Balling (Aarhus University, Department of Physics and Astronomy) for bringing laser photoconductive switching and associated THz technology to my attention. I should also like to thank Pernille Klarskov Pedersen (Aarhus University, Department of Engineering) for valuable discussions regarding the general field of THz generation and describing the feasibility of detecting the signals predicted here.

References

1 K. Kutzner, *Thin Solid Films*, 1972, **14**, 49.
2 R. Balog, P. Cicman, N. C. Jones and D. Field, *Phys. Rev. Lett.*, 2009, **102**, 073003.
3 D. Field, O. Plekan, A. N. Cassidy, R. Balog, N. C. Jones and J. Dunger, *Int. Rev. Phys. Chem.*, 2013, **32**, 345.
4 Y.-J. Chen, G. Muñoz Caro, S. Aparicio, A. Jiménez-Escobar, J. Lasne, A. Rosu-Finsen, M. R. S. McCoustra, A. M. Cassidy and D. Field, Wannier-Mott Excitons in Nanoscale Molecular Ices, *Phys. Rev. Lett.*, 2017, **119**, 157703.
5 J. Lasne, A. Rosu-Finsen, A. M. Cassidy, M. R. S. McCoustra and D. Field, *Phys. Chem. Chem. Phys.*, 2015, **17**, 20971–20980.
6 J. Lasne, A. Rosu-Finsen, A. M. Cassidy, M. R. S. McCoustra and D. Field, *Phys. Chem. Chem. Phys.*, 2015, **17**, 30177–30187.
7 M. Roman, S. Taj, M. Gutowski, M. R. S. McCoustra, A. C. Dunn, Z. G. Keolopile, A. Rosu-Finsen, A. M. Cassidy and D. Field, *Phys. Chem. Chem. Phys.*, 2018, **20**, 5112–5116.
8 A. M. Cassidy, R. L. James, A. Dawes, J. Lasne and D. Field, *Phys. Chem. Chem. Phys.*, 2019, **21**, 1190.
9 A. M. Cassidy, M. R. V. Jørgensen, A. Rosu-Finsen, J. Lasne, J. H. Jørgensen, A. Glavic, V. Lauter, B. B. Iversen, M. R. S. McCoustra and D. Field, *J. Phys. Chem. C*, 2016, **120**, 24130–24136.
10 A. M. Cassidy, D. Field, M. R. V. Jørgensen, A. Glavic and V. Lauter, 2019, to be submitted.
11 P. U. Jepsen, D. G. Cooke and M. Koch, *Laser Photonics Rev.*, 2011, **5**, 124.
12 A. Anderson and S. H. Walmsley, *Mol. Phys.*, 1964, **7**, 583.
13 J. E. Cahill and G. E. Leroi, *J. Chem. Phys.*, 1969, **51**, 1324.
14 K. R. Witters and J. E. Cahill, *J. Chem. Phys.*, 1977, **67**, 2405.
15 P. F. Krause and H. B. Friedrich, *Chem. Phys. Lett.*, 1973, **18**, 186.
16 A. M. Cassidy, R. L. James and D. Field, in preparation.
17 C. Kittel, *Introduction to Solid State Physics*, John Wiley&Sons, New York, London, Sydney, 3rd edn, 1968.
18 A. Natan, L. Kronik, H. Haick and R. T. Tung, *Adv. Mater.*, 2007, **19**, 4103.
19 J. Topping, *Proc. R. Soc. London, Ser. A*, 1927, **114**, 67.
20 A. M. Cassidy, O. Plekan, R. Balog, J. Dunger and D. Field, *J. Phys. Chem.*, 2014, **118**, 6615–6621.
21 D. J. Griffiths, *Introduction to Electrodynamics*, Pearson, 4th edn, 2013.
22 A. Dawes, M. Pascual, S. V. Hoffmann, N. C. Jones and N. J. Mason, *Phys. Chem. Chem. Phys.*, 2017, **19**, 27544.
23 See for example http://www.phys.boun.edu.tr/~sevgena/p202/docs/Electric%20dipole%20radiation.pdf.
24 F. J. Rodriguez-Fortuño, G. Marino, P. Ginzburg, D. O'Connor, A. Martinez, G. A. Wurtz and A. V. Zayats, *Science*, 2013, **340**, 328.
25 A. Yariv, *Quantum Electronics*, John Wiley and Sons, NY, 1988.
26 J. H. Hannay and D. Field, *Nature*, 1988, **333**, 540.
27 A. M. Cassidy, O. Plekan, J. Dunger, R. Balog, N. C. Jones, J. Lasne, A. Rosu-Finsen, M. R. S. McCoustra and D. Field, *Phys. Chem. Chem. Phys.*, 2014, **16**, 23843.
28 F. Simoens, THz Bolometer Detectors, in *Physics and Applications of Terahertz Radiation*, ed. M. Perenzoni and D. Paul, Springer Series in Optical Sciences, Springer, Dordrecht, 2014, vol. 173.
29 L. Duvillaret, F. Garet, J.-F. Roux and J.-J. Coutaz, *IEEE J. Sel. Top. Quantum Electron.*, 2001, **7**, 615.
30 N. Vieweg, F. Rettich, A. Deninger, H. Roehele, R. Dietz, T. Göbel and M. Schell, *J. Infrared, Millimeter, Terahertz Waves*, 2014, **35**, 823.
31 S. Yoshida, K. Suizi, E. Kato, Y. Nakagomi, Y. Ogawa and K. Kawase, *J. Mol. Spectrosc.*, 2009, **256**, 146.
32 M. Tonouchi, *Nat. Photonics*, 2007, **1**, 97.
33 M. M. Assefzadeh and A. Babakhani, *IEEE, J. Solid State Circ.*, 2017, **52**, 2905.
34 G. Scalari, C. Walther, M. Fischer, R. Terazzi, H. Beere, D. Titchie and J. Faist, *Laser Photonics Rev.*, 2009, **3**, 45.

